Formation of Multi-Component Star Structures at the Liquid/Solid Interface

Kazukuni Tahara,[†,] Kyohei Kaneko,[†] Keisuke Katayama,[†] Shintaro Itano,[†] Chi Huan Nguyen,[†] Deborah D. D. Amorim,[†] Steven De Feyter,[‡,]* Yoshito Tobe[†,]**

[†]Division of Frontier Materials Science, Graduate School of Engineering Science, Osaka University, Toyonaka, Osaka 560-8531, Japan and [‡]Division of Molecular Imaging and Photonics, Department of Chemistry, KU Leuven, Celestijnenlaan 200 F, 3001 Leuven, Belgium.

ABSTRACT

To demonstrate key roles of multiple interactions between multiple components and multiple phases in the formation of an uncommon self-assembling pattern, we present here the construction of a porous hexagonal star (*h*-star) structure using a trigonal molecular building block at the liquid/solid interface. For this purpose, self-assembly of hexaalkoxy substituted dehydrobenzo[12]annulene derivatives **DBA-OCn**s was investigated at the tetradecane/graphite interface by means of scanning tunneling microscopy (STM). Monolayer structures were significantly influenced by co-adsorbed tetradecane molecules depending on the alkyl chains length (C_{13}–C_{16}) of **DBA-OCn**. However, none of **DBA-OCn** molecules formed the expected trigonal complexes, indicating that an additional driving force is necessary for the formation of the trigonal complex and its assembly into the *h*-star structure. As a first approach, we employed the "guest induced structural change" for the formation of the *h*-star structure. In the presence of two guest molecules, non-substituted DBA and hexakis(phenylethynyl)benzene which fit the respective pores, an *h*-star structure was formed by **DBA-OC15** at the tetradecane/graphite interface. Moreover, a tetradecane molecule was co-adsorbed between a pair of alkyl chains of **DBA-OC15**, thereby blocking the interdigitation of the alkyl chain pairs. Therefore the *h*-star structure results from the cooperative self-assembly of the four molecular components including the solvent molecule. The second approach is based on aggregation of perfluoroalkyl chains via fluorophilicity of **DBA-F**, in which the perfluoro alkyl groups are substituted at the end of three alkyl chains of **DBA-OCn** via *para*-phenylene linkers. A trigonal complex consisting of **DBA-F** and three tetradecane molecules formed an *h*-star structure, in which the perfluoroalkyl groups that orient into the alkane solution phase aggregated at the hexagonal pore via fluorophilicity. The

present result provides useful insight into the design and control of complex molecular self-assembly at the liquid/solid interface.

INTRODUCTION

Self-assembled monolayers formed by organic molecules on solid surfaces have attracted a great deal of interest because of their potential to functionalize surfaces.[1–4] Two-dimensional (2D) molecular self-assemblies consisting of multiple components are relevant in connection with potential applications such as molecular-scale electronics, sensing, and catalysis, which require control over molecular organization of multiple components with nanometer precision. In particular, for the construction of complex, hierarchical structures control over intermolecular interactions between multiple components is indispensable. Though many examples of two- or three-component monolayers are known,[5–16] only a few reports have demonstrated the construction of four-component monolayers.[17,18] Thus, further development of robust strategies is important for successful construction of multi-component molecular self-assemblies on solid surfaces. Scanning tunneling microscopy (STM) is a powerful tool to characterize such structures on atomically flat conductive surfaces under UHV conditions or at the liquid/solid interface.

Over the past decade, we studied the self-assembly of trigonal building blocks, alkoxy-substituted dehydrobenzo[12]annulene (DBA) derivatives **DBA-OCn**s, at the liquid/solid interface (Figure 1). For instance, **DBA-OCn**s formed honeycomb type porous structures at the 1,2,4-trichlorobenzene (TCB)/graphite interface (Figure 2).[19,20] The key to selective formation of surface-confined honeycomb patterns, i.e. a regular array of nanowells, for this kind of compounds is the presence of van der Waals linkages between the interdigitated alkyl chains. Note that the relative alignment of the interdigitated alkyl chains in a pair of DBA molecules produces a chiral – or + type interdigitation motif. A chiral virtual 'clockwise' or 'counterclockwise' hexagonal pore

is formed by combining six – or + type interdigitation motifs, respectively (Figure 2a).[21] Distorted hexagonal pores are formed when + and – type interdigitation motifs are mixed in a hexagonal pore (Figure 2b).[21,22] The nanowells in those networks were often occupied by a variety of guest molecules forming multi-component monolayers.[12,16,23] The monolayer structure and its relative stability vary depending on the solvents employed.[19] For example, TCB favors the formation of the honeycomb structures most likely due to stabilization by solvent co-adsorption.[24,25]

Alkanes employed as low volatility solvents for monolayer preparation at liquid/solid interfaces are often co-adsorbed too in self-assembled monolayers of alkyl-substituted aromatic molecules forming multi-component network structures.[26–29] Therefore we conjectured that the intermolecular alkyl chain interdigitations between pairs of alkyl chains of adjacent molecules of a DBA derivative could be blocked efficiently by incorporation of a straight-chain alkane molecule into the alkyl chain pair, leading to the formation of a trigonal **DBA-OC*n***-alkane complex (Figure 2). Tiling of this trigonal complex is intriguing, because it should result in the formation of porous trigonal star (*t*-star), hexagonal, and hexagonal star (*h*-star) structures of *p*3, *p*6, or *p*6 symmetry, respectively. These plain groups appear in low frequencies in the Two-Dimensional Structural Database (1.4% and 2.2% for *p*3 and *p*6 plane groups, respectively).[31] Moreover, these porous patterns could template the co-adsorption of guest molecules, leading to construction of multi-component 2D structures.[32–34] The *t*-star structure consists of parallel arrays of the trigonal complexes whose alkyl ends converge, forming large hexagonal and small triangular pores (Figure 2c). In the hexagonal structure, each trigonal complex occupies the corners of a hexagon and the alkyl chain including the flanked alkane molecules align side-by-side, thus forming a hexagonal pore (Figure 2d). Similar to the hexagonal pattern, the trigonal complexes are aligned in a hexagonal manner but with their alkyl ends converged to form the *h*-star structure which contains

pores of different shape and size, i.e. large rhombic and small hexagonal pores (Figure 2e). This structure would therefore template the formation of multi-component monolayers by co-adsorption of different guest molecules at both types of pores. In contrast to the commonly observed packing patterns of trigonal molecules,[35–37] the *h*-star structure was reported only in a few instances.[38–40] For example, Matzger et al. reported that alkoxy benzamide formed an *h*-star structure at the 1-phenyloctane/graphite interface.[38,39] One of the driving forces for the formation of this structure is co-adsorption of solvent molecules at the pores. Recently, Kikkawa et al. reported the formation of an *h*-star structure consisting of a bimolecular mixture of isobutenyl ether compounds, though the driving force to form this pattern is not known.[40] The reasons for rare occurrence of this pattern are (i) a low molecular surface density and (ii) weak intermolecular interactions between the building blocks compared to those in other structures because of small van der Waals contacts.

On the basis of these considerations, we became interested in the construction of an *h*-star structure by controlling the spacing arrangement of the trigonal complex (Figure 2), by stabilizing the porous pattern via co-adsorption of guest molecules which fit in the individual pore space.[41] *n*-Tetradecane was chosen as a linear alkane molecule because this molecule is often used as a low volatile solvent for the monolayer preparations at the liquid/solid interface. STM investigations of the self-assemblies of **DBA-OCn** (n = 13, 14, 15, and 16) at the tetradecane/graphite interface revealed that the tetradecane molecules play a significant role in the formation of the monolayer structures by co-adsorption. However, the expected trigonal complexes were not observed. On the other hand, in the presence of two kinds of guest molecules, non-substituted DBA hereby called **PDBA** and hexakis(phenylethynyl)benzene **HPEB**, an *h*-star structure was formed by **DBA-OC15**. The guest molecules induced the formation of the *h*-star structure consisting of the four components including the solvent molecule tetradecane.

Moreover, we tested a second approach to fabricate an *h*-star structure at the tetradecane/graphite interface, using **DBA-F**, a second generation DBA in which functional groups are attached to the end of the three alternating alkyl chains through phenylene linkages (Figure 1).[42] In **DBA-F**, fluoroalkane fragments (C_8F_{17}) are attached at the end of three alkyl chains. As a result, a fluorophilicity exerted between the fluoroalkane units, which are located at the hexagonal pore but orient into the alkane solution phase because of limited space, induces the formation of an *h*-star structure by self-assembly of **DBA-F** and three tetradecane molecules without using any guest molecules (Figure 3). By these different approaches we demonstrate key roles of multiple interactions between multiple components and hierarchical interactions between multiple phases in the formation of an uncommon 2D pattern that is otherwise not formed by the building block itself.

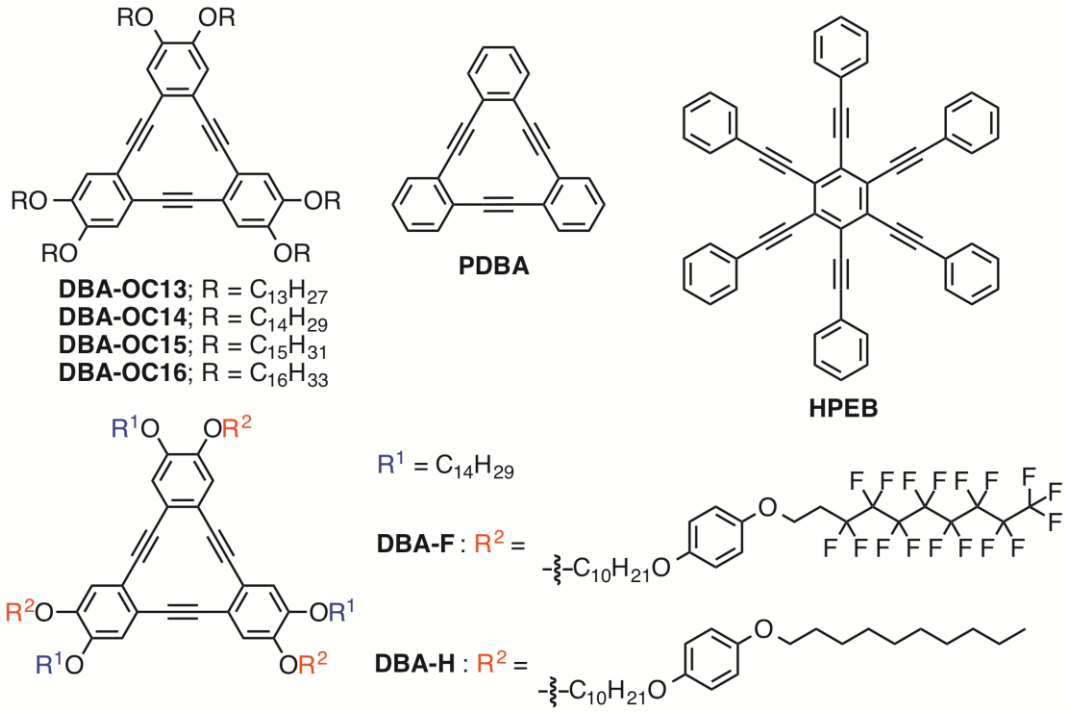

Figure 1. Chemical structures of **DBA-OCn**s, parent DBA **PDBA**, hexakis(phenylethynyl)benzene **HPEB**, **DBA-F**, and **DBA-H**.

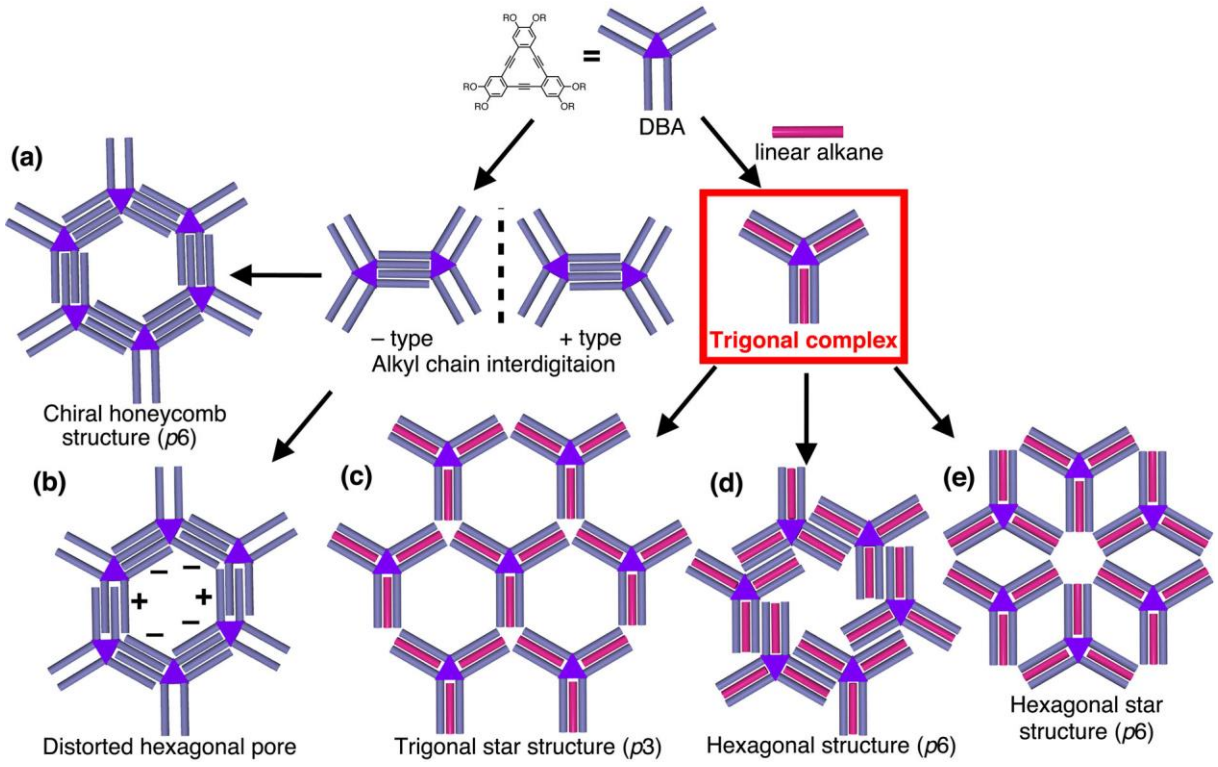

Figure 2. Schematic drawings representing self-assembly of (left) a dehydrobenzo[12]annulene (DBA) derivative and (right) the trigonal complex consisting of the DBA derivative and three molecules of a linear alkane each flanked by a pair of alkoxy chains of the DBA derivative. (left) The DBAs form chiral + and – type interdigitation motifs depending on the relative alignment of the four interdigitated alkyl chains per DBA pair. (a) A chiral regular hexagonal pore is formed by six chiral – or + type interdigitaion motif. (b) Combinations of the + and – type interdigitation motifs in an individual hexagonal pore produce distorted hexagonal pores. The trigonal complex forms three porous patterns, (c) a trigonal star structure (*t*-star), (d) a hexagonal structure, and (e) a hexagonal star structure (*h*-star). Magenta colored rods correspond to the linear alkanes which block intermolecular alkyl chain interdigitation between the DBAs.

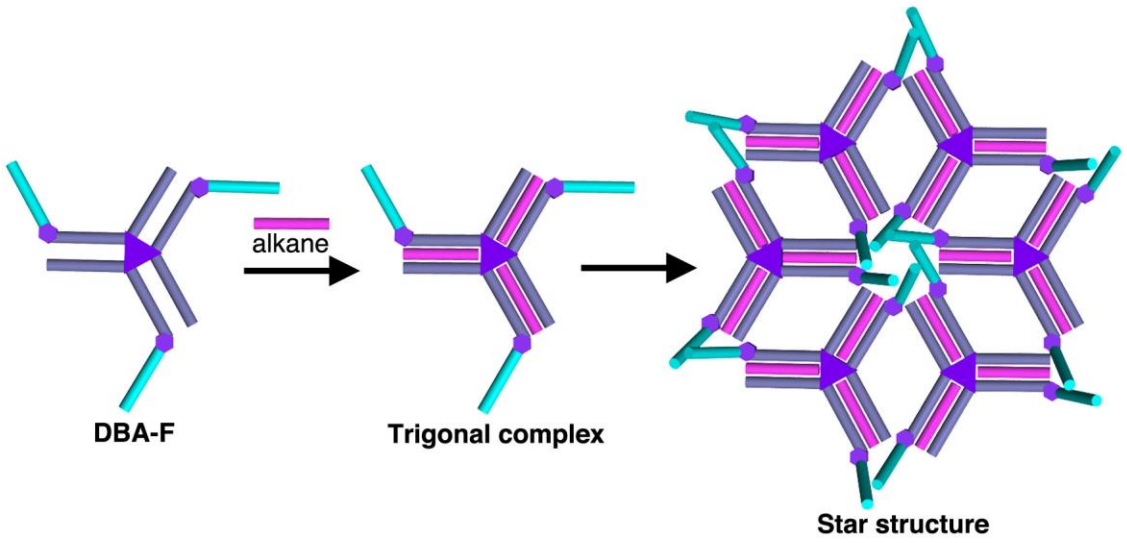

Figure 3. A schematic drawing representing the formation of a trigonal **DBA-F**-tetradecane complex and a hexagonal star (*h*-star) structure consisting of the trigonal complex. We expect that this structure is formed by fluorophilicity due to the segregated cluster of fluoroalkane units which stick out to the solution phase over the hexagonal pores.

EXPERIMENTAL SECTION

Synthesis of all DBA molecules were reported previously.[19,42,43] Parent DBA and hexakis(phenylethynyl)benzene were synthesized according to previous reports.[44,45] Commercially available tetradecane (TCI) was used for STM experiments.

All STM experiments were performed at 20–26 °C using a Nanoscope IIIa or IIID (Bruker AXS) with an external pulse/function generator (Agilent 33220A). Tips were mechanically cut from Pt/Ir wire (80%/20%, diameter 0.25 mm).

Prior to imaging, DBA derivative and guest molecules were dissolved in tetradecane. When more than two components were used, all components were mixed before STM investigations. Concentrations of each component are described in Figure captions. A drop of this solution was applied on a freshly cleaved surface of HOPG (grade ZYB, Momentive Performance Material

Quartz Inc., Strongsville, OH). All STM observations were performed at the tetradecane/graphite interfaces at room temperature. By changing the tunneling parameters during the STM imaging, namely, the voltage applied to the substrate and the average tunneling current, it was possible to switch from the visualization of the adsorbate layer to that of the underlying HOPG substrate. This enabled us to correct for drift effects by the use of SPIP software (Image Metrology A/S). The white colored axes shown in Figures indicate the direction of main symmetry axes of graphite underneath the molecular layers.

Each starting structure used for the MM simulation was built from the respective molecular model, whose structure was optimized by the PM3 method with a Gaussian 09 package.[46] Then, the orientation of the alkyl chains relative to the π-system was adjusted based on that observed in the STM images. The molecules were placed 0.350 nm above the first layer of an ideal two-layer graphite sheet (interlayer distance of graphite is 0.335 nm). Material Studio v7.0 software (Accelrys Software Inc.) was used for the geometry optimizations. All simulations were performed using COMPASS force field under an identical periodic boundary condition (a = b = 63.947 Å and γ = 60.000°). The graphite structure was frozen during the simulations, and a cutoff of 1.85 nm was applied for the vdW interactions.

RESULT AND DISSCUSSION

Self-Assemblies of DBA-OCn at the Tetradecane/Graphite Interface

First the monolayers of **DBA-OCn**s (n = 13, 14, 15, and 16) having alkoxy chains of approximately the same length as tetradecane (ca. 1.8 nm) were examined at the tetradecane/graphite interface to evaluate the formation of trigonal complexes by incorporation of tetradecane molecules between the paired alkyl chains of DBAs. Solute concentrations were set to 1.0–1.5 $\times 10^{-6}$ M to secure the formation of low molecular density phases.[47]

In the case of **DBA-OC13**, large domains consisting of distorted hexagonal pores were observed (Figure S1a). On the basis of a molecular model, we consider that the distorted hexagonal pores were stabilized by co-adsorbed tetradecane molecules which pack in the pores (Figure S1b). Incorporation of a tetradecane molecule in the paired alkyl chains was observed only at domain boundaries or network defects. In contrast, formation of regular honeycomb domains was observed for **DBA-OC14** and **DBA-OC15** (Figures S2a and 4a). It should be noted that linear rows of an extended honeycomb pore or an offset honeycomb structure were occasionally observed in the honeycomb domains of both compounds (Figures S2b,c and 4c,d). In these irregular structures, the interdigitation of the alkyl chains of adjacent DBA molecules was blocked by incorporation of a tetradecane molecule between the paired alkyl chains of the DBA molecule. In the extended honeycomb pattern, hemi-hexagonal units contact each other at the tails, whereas in the offset honeycomb form, they contact in a side-by-side mode. The co-adsorbed tetradecane molecules at the open space of these low density structures appear to stabilize the self-assembled structure. In the case of **DBA-OC16**, domains consisting of linearly aligned molecular rows appeared as the dominant form (Figure 5a). In this structure, two of the three paired alkyl chains of a DBA molecule are blocked by incorporation of tetradecane molecules, whereas the third alkyl chain pair

forms an intermolecular linkage to a neighboring DBA molecule to form a dimer (Figures 5b,c). Additional tetradecane molecules occupy the open spaces. Moreover, rows of hexagonal structures of the trigonal complex (Figure 2d) were observed at domain boundaries (Figures 5b,d). In contrast to the DBAs with shorter alkyl chains, the honeycomb structure was observed scarcely. To estimate the probability of blocking by tetradecane to the alkyl chain interdigitation between these DBAs, we performed a statistical analysis of the numbers of the interdigitated or the blocked alkyl chain pairs of DBAs in more than four STM images. The probability that tetradecane adsorption blocks alkyl chain interdigitation are 7% for **DBA-C13**, 10% for **DBA-OC14**, 11% for **DBA-OC15**, and 63% for **DBA-OC16**.

To elucidate structural differences and intermolecular interactions at a single molecular level, size matching between tetradecane and alkyl chains of **DBA-OCn** and their intermolecular interactions were examined by molecular mechanics simulations based on trigonal complexes consisting of one molecule of **DBA-OCn** (n = 13–16) and three tetradecane molecules (magenta, Figure 6) on a bilayered graphene sheet. In the case of **DBA-OC13**, the incorporated tetradecane molecule is apparently longer than the OC13 chains. The incorporated tetradecane molecule is still slightly longer than the OC14 chains of **DBA-OC14**. In the case of **DBA-OC15**, the length of a tetradecane molecule fits that of the OC15 chains. The length of tetradecane is shorter than that of the paired alkyl chains of **DBA-OC16**. Intermolecular interactions proportionally increase by the elongation of the alkoxy chains of **DBA-OCn**s (Table S1). However there was no obvious energy differences which accounted for the highest probability of blocking observed in **DBA-OC16**.

We suggest that co-adsorption of the solvent molecules at open spaces (i.e. network pore) plays a significant role in determining the probabilities of the blocking by tetradecane and monolayer structures of **DBA-OCn**s. For instance, co-adsorbed tetradecane molecules stabilize the distorted

hexagonal pore made by **DBA-OC13** (Figure S1). Therefore, the blocking was observed only at the domain boundary and the probability of blocking remained 7%. In the cases of **DBA-OC14** and **DBA-OC15**, the regular hexagonal pore, the extended honeycomb pore, and the offset honeycomb structure are also stabilized by co-adsorbed tetradecane molecules (Figures 4b–d). Therefore, the probabilities of blocking are slightly increased (10–11%) for these two systems. On the other hand, honeycomb structures were not formed by **DBA-OC16** because tetradecane molecules would not pack within the hexagonal pores. Instead, **DBA-OC16** formed the domains of the linearly aligned molecular rows by co-adsorption of the tetradecane molecules at the open space with the highest probability of blocking (63%). These results however indicated that trigonal complexes were not formed, expect for the hexagonal structure of **DBA-OC16** (Figures 5b,d), by tetradecane alone. An *h*-star structure was never observed either, indicating that an additional driving force is required for the formation of the trigonal complexes and to drive them to form an *h*-star structure.

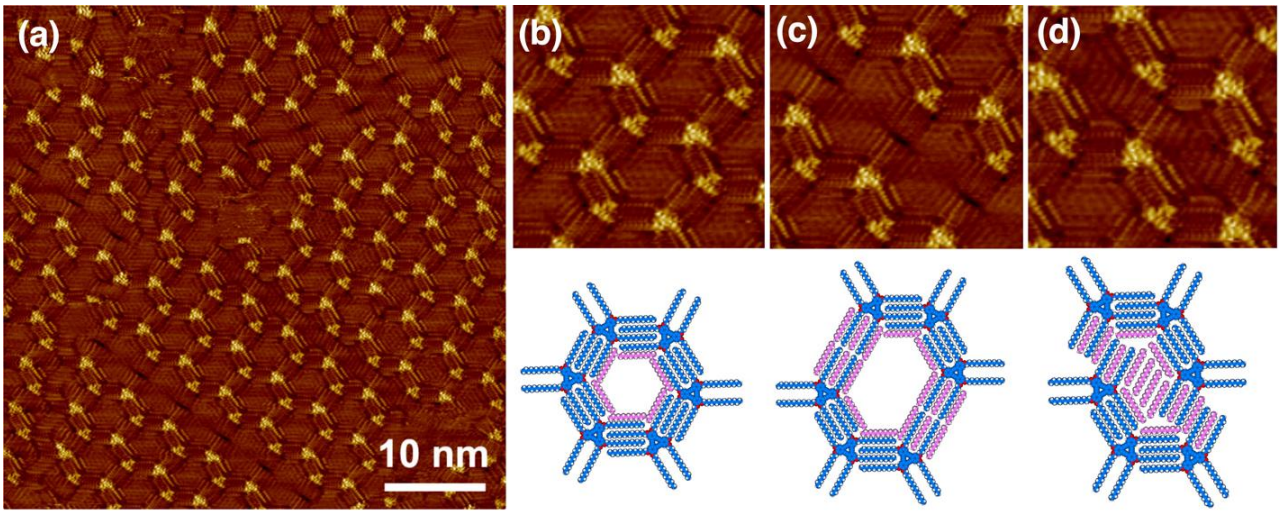

Figure 4. STM images and molecular models of monolayers consisting **DBA-OC15** at the tetradecane/graphite interface (concentration; 1.5×10^{-6} M, tunneling parameters; I_{set} = 0.22 nA,

V_{set} = –0.35 V for all images). (a) Large area image. (b) Enlarged image of the honeycomb structure. (c) Enlarged image of the extended pore. (d) Enlarged image of the offset structure.

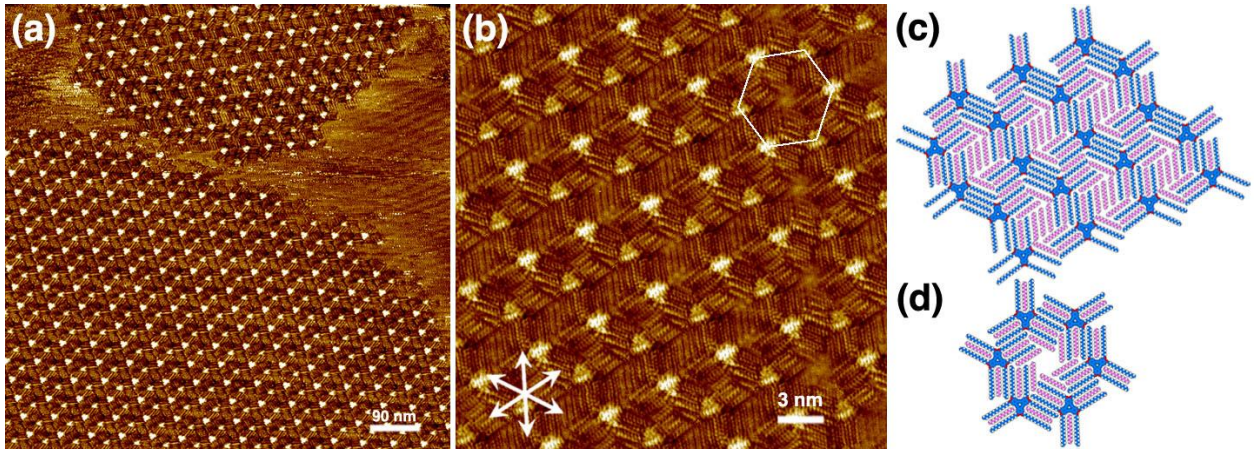

Figure 5. (a, b) STM images of monolayers consisting of **DBA-OC16** and tetradecane at the tetradecane/graphite interface (concentration; 1.0×10^{-6} M, tunneling parameters; I_{set} = 0.05 nA, V_{set} = –0.21 V for both images). In the image (b), there are hexagonal structures, one of which is highlighted by a white hexagon, in the right side of the image. (c, d) Models of the domains consisting of linearly aligned molecular rows (c) and the hexagonal structure (d).

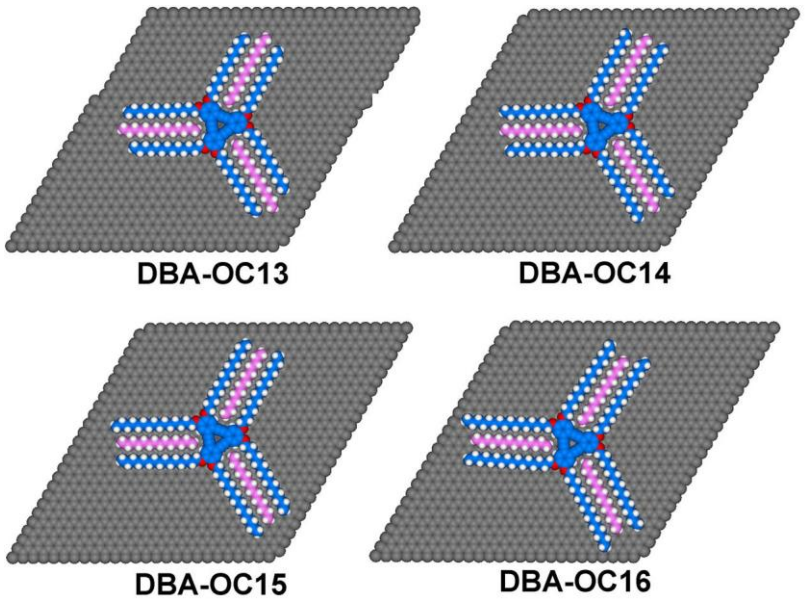

Figure 6. Molecular models of the trigonal complexes consisting of **DBA-OCn** (n = 13–16, blue) and tetradecane molecules (magenta) optimized by molecular mechanics simulation (COPASS force field) on a bilayered graphite sheet under an identical periodic boundary condition (a = b = 63.947 Å and γ = 60.000°).

Guest-Induced Formation of Hexagonal Star Structure

It is known that guest molecules induce structural transformation from non-porous patterns to porous forms by templating the latter through an induced-fit mechanism.[16,23,48,49] The main driving forces for this phenomenon are van der Waals interactions between a guest and the solid substrate surface and van der Waals interactions between a guest and the surrounding host matrix. For the later interactions, shape and size complementarity between the guest and the pore plays a crucial role. In this respect, we performed a molecular model study for the targeted *h*-star structure bearing a hexagonal and six rhombic pores as a basic motif (Figure 7). For the prospective *h*-star structure, the size and shape of **HPEB** and a dimer of **PDBA** should fit the respective pores formed by the trigonal complex of **DBA-OC15** and three tetradecane molecules (Figure 7b). As shown in Figures 7a,c, the modeling study also suggests that the pores formed by **DBA-OC14** are too small for both guest molecules, whereas the pores formed by **DBA-OC16**, particularly the rhombic one, are too large. On the basis of the above modeling, we investigated 2D self-assemblies formed by **DBA-OC15**, **HPEB**, and **PDBA** at the tetradecane/graphite interface. First we studied the influence of the mixing ratio of the three components on the 2D pattern formation using a premixed solution in tetradecane (Table S2). As a result, co-existence of both the *h*-star and honeycomb structures was found at the following concentrations; 1.5×10^{-6} M for **DBA-OC15**, 1.0×10^{-3} M for **PDBA** and 5.4×10^{-7} M for **HPEB** (3 to 4100 to 1 in molar ratio). Figure 8 displays a high resolution STM image and the corresponding molecular model of the *h*-star structure. The dim lines between the

paired alkyl chains of **DBA-OC15** correspond to co-adsorbed tetradecane molecules revealing the formation of the trigonal complex. The two bright triangular features in the rhombic pores are **PDBA** molecules, and the bright asterisks in the hexagonal pores correspond to immobilized **HPEB** molecules. Note that the *h*-star structure is chiral as a consequence of a small offset in the relative positions of the pair of **PDBA** molecules in the rhombic pore. Indeed, there exists an antipodal pattern in different domains (Figure S3). In the honeycomb structures, the pores were imaged as fuzzy bright features indicating co-adsorption of mobile guest molecules (Figure S4). The populations calculated from 16 large area STM images (60 nm × 60 nm) were 43% and 57% for the *h*-star and honeycomb structures, respectively.

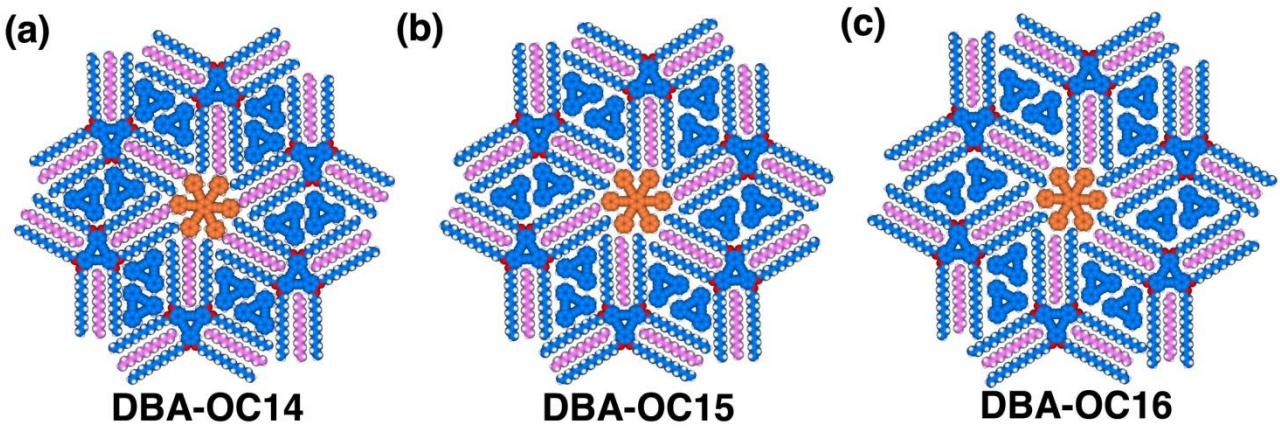

Figure 7. Molecular models of the four-component *h*-star structures consisting of **DBA-OCn**, tetradecane (magenta), **PDBA** (blue), and **HPEB** (orange). (a) **DBA-OC14**, (b) **DBA-OC15**, and (c) **DBA-OC16**. **DBA-OCn**, tetradecane, **PDBA** and **HPEB** molecules were independently optimized by PM3 method under vacuum. The orientations of the alkoxy chains of **DBA-OCn** were adjusted to form trigonal complexes with tetradecane molecules.

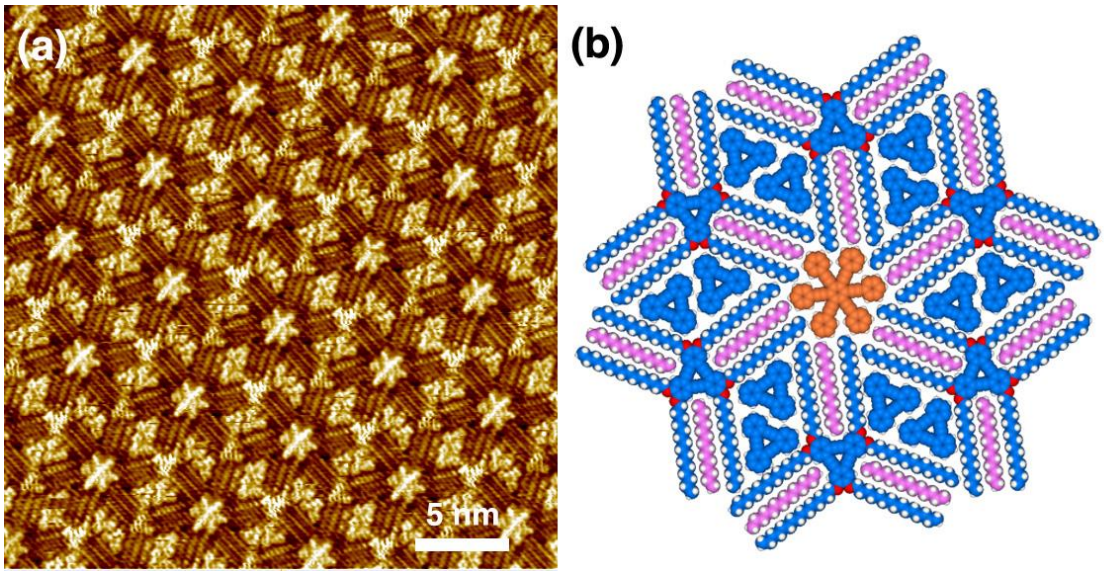

Figure 8. STM image (a) and a molecular model (b) of the four-component self-assembly formed by dropping a solution of a mixture of **DBA-OC15**, **PDBA**, and **HPEB** in tetradecane on graphite (concentrations; 1.5×10^{-6} M for **DBA-OC15**, 1.0×10^{-3} M for **PDBA**, and 5.4×10^{-7} M for **HPEB**, tunneling parameters; $I_{set} = 0.30$ nA, $V_{set} = -0.27$ V). Unit cell parameters are a = 5.8 ± 0.1 nm, b = 5.8 ± 0.1 nm, γ = 59.9 ± 0.4°. In the model (b), magenta and orange colored molecules are tetradecane molecules and **HPEB**, respectively.

Control experiments confirmed that all four components were necessary for the *h*-star structure formation. Indeed, a mixture of **DBA-OC15** and **PDBA** produced a honeycomb structure of **DBA-OC15** where the pores were imaged as fuzzy features indicating the co-adsorption of mobile **PDBA** molecules (Figure S5). Only at domain boundaries, rhombic pores filled with paired **PDBA** molecules were observed occasionally (blue arrows in Figure S5b). Similarly, a honeycomb structure appeared for a mixture of **DBA-OC15** and **HPEB** (Figure S6). While most of the pores were filled with co-adsorbed tetradecane molecules, fuzzy features were observed at a few pores

suggesting the co-adsorption of **HPEB** molecules (blue arrows in Figure S6). More importantly, all attempts to observe the *h*-star structures from **DBA-OC14** and **DBA-OC16** in the presence of **PDBA** and **HPEB** (Figure S7) were never successful. These mixtures exhibited disordered structures and a small proportion of honeycomb structures, being consistent with the predictions based on the modeling studies.

Though several examples of formations of 2D self-assemblies are known for two- and three-component systems,[5–17] only one example was reported by Zimmt et al. for a four-component system.[18] In this case, a kinked diacetylene (DA) unit in alkyl chains linked to anthracene cores controls the order of four different molecules aligned in 1D rows via steric complementarity of the DA units.[18] In contrast to Zimmt's work, a key factor for the formation of the present four-component structure is the recognition of size and shape between the pores and co-adsorbed guest molecules including tetradecane solvent molecules inserted between the paired alkyl chains of a DBA derivative. Another characteristic in the present four-component system is that the *h*-star structure is different from the monolayer pattern (i.e., disordered or honeycomb structures) formed by the host only or by the host and guest molecule(s). In addition, the present system differs from our previous examples of the three- or four-component structure using **DBA-OC10** or a related rhombus molecule as a host molecule, in which the host porous networks were constructed without addition of guest molecules by interdigitation of the alkyl chains attached to the host molecules.[12,17]

Formation of Hexagonal Star Structure by Fluorophilicity

In addition to the formation of the *h*-star structure induced by cooperative adsorption of a host, i.e. two kinds of guests, and solvent molecules, we describe here an approach for the formation of an *h*-star structure which is driven by fluorophilicity. In general, homogeneous mixing of liquid

alkanes and fluoroalkanes is highly disfavored due to the inequality of the cohesive energy densities.[50–56] Moreover, fluorinated segments in molecules tend to aggregate by themselves, often showing phase segregation at the supramolecular level, which has been utilized in designing molecular self-assemblies.[57] We recently reported fluorophilicity-driven guest recognition at the functionalized 2D pore of a honeycomb structure formed by **DBA-F** (Figure 1), a second generation DBA having perfluoroalkyl groups at the end of the three OC14 chains connected with *para*-phenylene linkers, at the 1-phenyloctane/graphite interface.[42] In this context, we are interested in the self-assembling property of **DBA-F** if three tetradecane molecules are inserted into its three pairs of C14-alkoxy groups. More specifically, an *h*-star structure could be formed taking into account the fact that in the prospective *h*-star structure the perfluoroalkane units of six trigonal **DBA-F**-tetradecane complexes would be located in close proximity, thereby forming a segregated cluster by fluorophilicity (Figure 3). In the segregated cluster, the fluoroalkane units are expected to orient to a solution phase due to space limitation. On the basis of the above conjecture, the self-assembly of **DBA-F** was investigated at the tetradecane/graphite interface.

Figure 9a displays an STM image of a monolayer formed by **DBA-F** at the tetradecane/graphite interface. The surface was exclusively covered by a *h*-star structure of **DBA-F** (Figure 9b). In the image, trigonal complexes consisting of the C14 alkoxy chains of **DBA-F** and tetradecane are clearly visible. Moreover, small bright single dots located at the corners of the hexagonal pores correspond to the phenylene linkers. The center of the hexagonal pores was imaged fuzzy indicating that the fluoroalkane units orient to the tetradecane solution phase (Figure 9c). Two tetradecane molecules were clearly observed at the rhombic pores. The size and shape of two tetradecane molecules nicely fits the smaller rhombic pore surrounded by the OC14 chains of **DBA-F**. It should be pointed out that in contrast to the case of **DBA-OC15**, the *h*-star structure

was formed from **DBA-F** without any guest molecules, because tetradecane molecules served as guests to occupy the rhombic pores. To clarify the effect of fluoroalkyl groups, self-assembly of **DBA-H** having terminal C10 alkyl chains instead of the perfluoroalkyl groups (Figure 1) was examined under identical experimental conditions. However, it formed a honeycomb structure together with disordered structures similar to those observed in 1-phenyloctane,[42] and an *h*-star structure was never observed (Figure S8).

These results together with the observed *h*-star structure of **DBA-F** strongly indicate that stabilization due to the aggregation of the perfluoroalkane units via fluorophilicity plays a crucial role for the formation of the *h*-star structure. In other words, the *h*-star structure was formed via hierarchical interactions in multiple phases, one on surface and the other in solution.

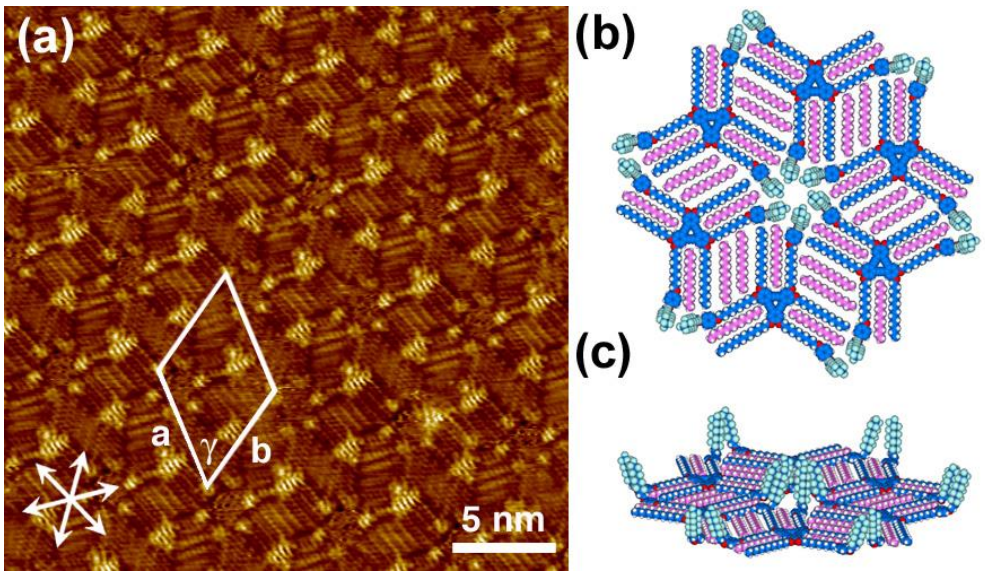

Figure 9. STM image (a) and molecular models (b, c) of the *h*-star structure consisting of **DBA-F** at the tetradecane/graphite interface (concentration; 3.0×10^{-6} M, I_{set} = 0.19 nA, V_{set} = –0.29 V). Unit cell parameters are a = 5.8 ± 0.3 nm, b = 5.7 ± 0.2 nm, γ = 60 ± 1°. In the models (b, c), the

fluoroalkyl chains of **DBA-F** are colored in turquoise. Magenta colored molecules are co-adsorbed tetradecane molecules.

CONCLUSION

In summary, we have investigated 2D self-assemblies of DBA derivatives at the tetradecane/graphite interface aiming at evaluating the blocking effect of co-adsorbed solvent molecules on the interdigitation of alkyl chains pairs of adjacent molecules. As a result, we observed two cases of *h*-star structures formed by trigonal complexes consisting of the DBA derivative and three tetradecane molecules inserted into each of the three pairs of alkyl chains of the DBA. In the first instance, **DBA-OC15** formed the star structure in the presence of two different guest molecules, **HPEB** and **PDBA**, as a consequence of the self-assembly of the four molecular components including the solvent molecule. A main factor for the formation of the *h*-star structure is the size and shape complementarity between the pores formed by the trigonal complex. The second case we observed is the self-assembly of **DBA-F** having perfluoroalkyl groups at the end of the three alkoxy chains. In this case, tetradecane molecules are co-adsorbed at the rhombic pores in addition to the space between the paired alkyl chains of **DBA-F**. However, the most important factor for the formation of the *h*-star structure is the stabilization due to the aggregation of the perfluoroalkane units orient into the alkane solution phase via fluorophilicity. In both instances, it appeared that the host, guest, and solvent molecules act cooperatively to form the complex 2D patterns, provided that their size and shape fit each other by structural fine tuning.

The present results reveal two essential elements for the formation of the *h*-star structure: (1) multiple interactions between multiple components including solvent molecules on the surface and (2) hierarchical interactions in multiple phases, one on surface and the other in solution. These

information provides significant insight for the construction of complex, hierarchal 2D patterns consisting of multiple components, which is useful in the field of 2D crystal engineering.

SUPPORTING INFORMATION

Additional STM images, intermolecular interactions calculated by MM simulations. This material is available free of charge via the Internet at http://pubs.acs.org.

ACKNOWLEDGMENT

This work is supported by JSPS KAKENHI Grant Numbers 21245012, 24350046, and 26620063, the Fund of Scientific Research – Flanders (FWO), KU Leuven (GOA 2011/2), and the Hercules Foundation, the Belgian Federal Science Policy Office through IAP 7/05. This research has also received funding from the European Research Council under the European Union's Seventh Framework Programme (FP7/2007-2013)/ERC grant agreement no. 340324. C. H. N. and D. D. D. A. acknowledge the FrontierLab@OsakaU program for the support to their study at Osaka University.

REFERENCES

(1) Barth, J. V. *Annu. Rev. Phys. Chem.* **2007**, *58*, 375–407.

(2) Barth, J. V.; Costantini, G.; Kern, K. *Nature* **2005**, *437*, 671–679.

(3) Elemans, J. A. A. W.; Shengbin, L.; De Feyter, S. *Angew. Chem. Int. Ed.* **2009**, *48*, 7298–7332.

(4) Palma, C.-A.; Samorì, P. *Nat. Chem.* **2011**, *3*, 431–436.

(5) Eichhorst-Gerner, K.; Stabel, A.; Moessner, G.; Declerq, D.; Valiyaveettil, S.; Enkelmann, V.; Müllen, K.; Rabe, J. P. *Angew. Chem. Int. Ed.* **1996**, *35*, 1492–1495.

(6) Kampschulte, L.; Griessl, S.; Heckl, W. M.; Lackinger, M. *J. Phys. Chem. B* **2005**, *109*, 14074–14078.

(7) Nath, K. G.; Ivasenko, O.; Miwa, J. A.; Dang, H.; Wuest, J. D.; Nanci, A.; Perepichka, D. F.; Rosei, F. *J. Am. Chem. Soc.* **2006**, *128*, 4212–4213.

(8) Llanes-Pallas, A.; Matena, M.; Jung, T.; Prato, M.; Stöhr, M.; Bonifazi, D. *Angew. Chem. Int. Ed.* **2008**, *47*, 7726–7730.

(9) Shen, Y.; Deng, K.; Li, M.; Zhang, X.; Zhou, G.; Müllen, K.; Zeng, Q.; Wang, C. *CrystEngComm* **2013**, *15*, 5526–5531.

(10) Liu, J.; Chen, T.; Deng, X.; Wang, D.; Pei, J.; Wan, L.-J. *J. Am. Chem. Soc.* **2011**, *132*, 21010–21015.

(11) Theobald, J. A.; Oxtoby, N. S.; Phillips, M. A.; Champness, N. R.; Beton, P. H. *Nature* **2003**, *424*, 1029–1031.

(12) Lei, S.; Surin, M.; Tahara, K.; Adisoejoso, K.; Lazzaroni, R.; Tobe, Y.; De Feyter, S. *Nano Lett.* **2008**, *8*, 2541–2546.

(13) Shen, Y.-T.; Li, M.; Guo, Y.-Y.; Deng, K.; Zeng, Q.-D.; Wang, C. *Chem. Asian J.* **2010**, *5*, 787–790.

(14) Schull, G.; Douillard, L.; Fiorini-Debuisschert, C.; Charra, F.; Mathevet, F.; Kreher, D.; Attias, A.-J. *Nano Lett.* **2006**, *6*, 1360–1363.

(15) Stepanow, S.; Lingenfelder, M.; Dmitriev, A.; Spillmann, H.; Delvigne, E.; Lin, N.; Deng, X.; Cai, C.; Barth, J. V.; Kern, K. *Nature Mater.* **2004**, *3*, 229–233.

(16) Li, Y.; Ma, Z.; Deng, K.; Lei, S.; Zeng, Q.; Fan, X.; De Feyter, S.; Huang, W.; Wang, C. *Chem. Eur. J.* **2009**, *15*, 5418–5423.

(17) Adisoejoso, J.; Tahara, K.; Okuhata, S.; Lei, S.; Tobe, Y.; De Feyter, S. *Angew. Chem. Int. Ed.* **2009**, *48*, 7353–7357.

(18) Xue, Y.; Zimmt, M. B. *J. Am. Chem. Soc.* **2012**, *134*, 4513–4516.

(19) Tahara, K.; Furukawa, S.; Uji-i, H.; Uchino, T.; Ichikawa, T.; Zhang, J.; Mamdouh, W.; Sonoda, M.; De Schryver, F. C.; De Feyter, S.; Tobe, Y. *J. Am. Chem. Soc.* **2006**, *128*, 16613–16625.

(20) Tahara, K.; Lei, S.; Adisoejoso, J.; De Feyter, S.; Tobe, Y. *Chem. Commun.* **2010**, *46*, 8507–8525.

(21) Tahara, K.; Yamaga, H.; Ghijsens, E.; Inukai, K.; Adisoejoso, J.; Blunt, M. O.; De Feyter, S.; Tobe, Y. *Nature Chem.* **2011**, *3*, 714–719.

(22) Destoop, I.; Ghijsens, E.; Katayama, K.; Tahara, K.; Mali, K. S.; Tobe, Y.; De Feyter, S. *J. Am. Chem. Soc.* **2012**, *134*, 19568–19571.

(23) Furukawa, S.; Tahara, K.; De Schryver, F. C.; Van der Auweraer, M.; Tobe, Y.; De Feyter, S. *Angew. Chem. Int. Ed.* **2007**, *46*, 2831–2834.

(24) Tahara, K.; Okuhata, S.; Adisoejoso, J.; Lei, S.; Fujita, T.; De Feyter, S.; Tobe, Y. *J. Am. Chem. Soc.* **2009**, *131*, 17583–17590.

(25) Blunt, M. O.; Adisoejoso, J.; Tahara, K.; Katayama, K.; Van der Auweraer, M.; Tobe, Y.; De Feyter, S. *J. Am. Chem. Soc.* **2013**, *135*, 12068–12075.

(26) Chng, G. Y. Y.; Sun, X.; Cho, S. J.; Rajwar, D.; Grimsdale, A. C.; Fichou, D. *New J. Chem.* **2014**, *38*, 2407–2413.

(27) Miao, X.; Xu, L.; Li, Z.; Deng, W. *J. Phys. Chem. C* **2011**, *115*, 3358–3367.

(28) Shen, Y.; Deng, K.; Li, M.; Zhang, X.; Zhou, G.; Müllen, K.; Zeng, Q.; Wang, C. *CrystEngComm* **2013**, *15*, 5526–5531.

(29) Miao, X.; Xu, L.; Cui, L.; Deng, W. *Phys. Chem. Chem. Phys.* **2014**, *16*, 12544–12553.

(31) Plass, K. E.; Grzesiak, A. L.; Matzger, A. J. *Acc. Chem. Res.* **2007**, *40*, 287–293.

(32) Bonifazi, D.; Mohnani, S.; Llanes-Pallas, A. *Chem. Eur. J.* **2009**, *15*, 7004–7025.

(33) Kudernac, T.; Lei, S.; Elemans, J. A. A. W.; De Feyter, S. *Chem. Soc. Rev.* **2009**, *38,* 402–421.

(34) XueMei, Z.; QingDao, Z.; Chen, W. *Science China* **2014**, *57*, 13–25.

(35) Ciesielski, A.; Szabelski, P. J.; Rżysko, W.; Cadeddu, A.; Cook, T. R.; Stang, P. J.; Samorì, P. *J. Am. Chem. Soc.* **2013**, *135*, 6942–6950.

(36) Tsuji, H.; Cantagrel, G.; Ueda, Y.; Chen, T.; Wan, L.-J.; Nakamura, E. *Chem. Asian J.* **2013**, *8*, 2377–2382.

(37) Mu, Z.; Shu, L.; Fuchs, H.; Mayor, M.; Chi, L. *J. Am. Chem. Soc.* **2008**, *130*, 10840–10841.

(38) Ahn, S.; Morrison, C. N.; Matzger, A. J. *J. Am. Chem. Soc.* **2009**, *131*, 7946–7947.

(39) Ahn, S.; Matzger, A. J. *J. Am. Chem. Soc.* **2010**, *132*, 11364–11371.

(40) Kikkawa, Y.; Ishituka, M.; Kashiwada, A.; Tsuzuki, S.; Hiratani, K. *Chem. Commun.* **2014**, *50*, 13146–13149.

(41) Similar idea was demonstrated on a bimolecular self-assembly of alkoxylated truxcene derivative and 1,3,5-alkoxybenzene derivative having carboxy groups at the end of all chains. Liu, J.; Zhang, X.; Wang, D.; Wang, J.-Y.; Pei, J.; Stang, P. J.; Wan, L. J. *Chem. Asian. J.* **2011**, *6*, 2426–2430.

(42) Tahara, K.; Katayama, K.; Blunt, M. O.; De Feyter, S.; Tobe, Y. *ACS Nano* **2014**, *8*, 8683–8694.

(43) Ghijsens, E.; Ivasenko, O.; Tahara, K.; Yamaga, H.; Itano, S.; Balandina, T.; Tobe, Y.; De Feyter, S. *ACS Nano* **2013**, *7*, 8031–8042.

(44) Iyoda, M.; Sirinintasak, S.; Nishiyama, Y.; Vorasingha, A.; Sultana, F.; Nakao, K.; Kuwatani, Y.; Matsuyama, H.; Yoshida, M.; Miyake, Y. *Synthesis* **2004**, 1527–1531.

(45) Ehlers, P.; Neubauer, A.; Lochbrunner, S.; Villinger, A.; Langer, P. *Org. Lett.* **2011**, *13*, 1618–1621.

(46) Gaussian 09, Revision C.1, Frisch, M. J.; Trucks, G. W.; Schlegel, H. B.; Scuseria, G. E.; Robb, M. A.; Cheeseman, J. R.; Scalmani, G.; Barone, V.; Mennucci, B.; Petersson, G. A.; Nakatsuji, H.; Caricato, M.; Li, X.; Hratchian, H. P.; Izmaylov, A. F.; Bloino, J.; Zheng, G.; Sonnenberg, J. L.; Hada, M.; Ehara, M.; Toyota, K.; Fukuda, R.; Hasegawa, J.; Ishida, M.; Nakajima, T.; Honda, Y.; Kitao, O.; Nakai, H.; Vreven, T.; Montgomery, Jr., J. A.; Peralta, J. E.; Ogliaro, F.; Bearpark, M.; Heyd, J. J.; Brothers, E.; Kudin, K. N.; Staroverov, V. N.; Kobayashi,

R.; Normand, J.; Raghavachari, K.; Rendell, A.; Burant, J. C.; Iyengar, S. S.; Tomasi, J.; Cossi, M.; Rega, N.; Millam, J. M.; Klene, M.; Knox, J. E.; Cross, J. B.; Bakken, V.; Adamo, C.; Jaramillo, J.; Gomperts, R.; Stratmann, R. E.; Yazyev, O.; Austin, A. J.; Cammi, R.; Pomelli, C.; Ochterski, J. W.; Martin, R. L.; Morokuma, K.; Zakrzewski, V. G.; Voth, G. A.; Salvador, P.; Dannenberg, J. J.; Dapprich, S.; Daniels, A. D.; Farkas, Ö.; Foresman, J. B.; Ortiz, J. V.; Cioslowski, J.; Fox, D. J. Gaussian, Inc., Wallingford CT, 2009.

(47) Lei, S.; Tahara, K.; De Schryver, F. C.; Van der Auweraer, M.; Tobe, Y.; De Feyter, S. *Angew. Chem. Int. Ed.* **2008**, *47*, 2964–2968.

(48) Blunt, M.; Lin, X.; del Carmen Gimenez-Lopez, M.; Schröder, M.; Champness, N. R.; Beton, P. H. *Chem. Commun.* **2008**, 2304–2306.

(49) Bléger, D.; Kreher, D.; Mathevet, F.; Attias, A.-J.; Schull, G.; Huard, A.; Douillard, L.; Fiorini-Debuischert, C.; Charra, F. *Angew. Chem. Int. Ed.* **2007**, *46*, 7404–7407.

(50) Scott, R. L. *J. Am. Chem. Soc.* **1948**, *70*, 4090–4093.

(51) Bedford, R. G.; Dunlap, R. D. *J. Am. Chem. Soc.* **1959**, *81*, 2927–2930.

(52) Young, C. L. *Trans. Faraday Soc.* **1969**, *65*, 2639–2644.

(53) Mukerjee, P.; Handa, T. *J. Phys. Chem.* **1981**, *85*, 2298–2303.

(54) Mukerjee, P. *J. Am. Oil Chem. Soc.* **1982**, *59*, 573–578.

(55) Binks, B. P.; Fletcher, P. D. I.; Kotsev, S. N.; Thompson, R. L. *Langmuir* **1997**, *13*, 6669–6682.

(56) Dorset, D. L. *Macromolecules* **1990**, *23*, 894–901.

(57) Krafft, M. P.; Riess, J. G. *Chem. Rev.* **2009**, *109*, 1714–1792.

TOC Graphics

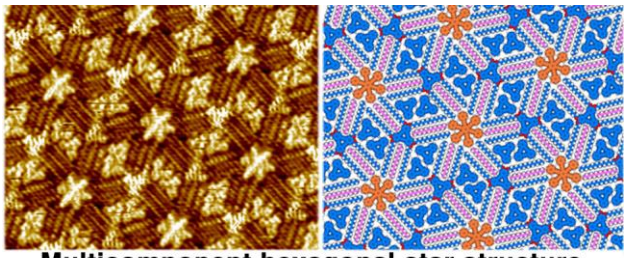

Multicomponent hexagonal star structure